

Lung Nodule Retrieval System

Gagan Deep
Department of CSE,
Chandigarh Engg. College
(CEC), Landran-140307,
Mohali, India.

Lakhwinder Kaur
Department of CE, UcoE,
Punjabi University, Patiala.

Savita Gupta
Department of CSE, UIET, PU,
Chandigarh.

ABSTRACT

Early detection and removal of pulmonary nodules significantly improves long term survival rates for patients with lung cancer. This paper provides the overview of different methods used in the retrieval system of lung nodules by a comprehensive review of existing literature. Firstly, the high level features of DICOM CT images are used for retrieval of filtered lung images from the database. The preprocessing step is used for separation of lungs fields on the filtered images. Linear Binary Pattern extracts the low level features from extracted lung areas to perform the segmentation. The technique of template matching further uses to retrieve the abnormal nodules from Lung data set.

Keywords

DICOM CT scans, lung nodules, high level features, low level features, LBP, template matching.

1. INTRODUCTION

Lung cancer is one of the most common causes of cancer in the United States [1]. It is the uncontrollable growth of abnormal cells in the lungs. In this paper, for identifying the lung nodules, DICOM [4] Computed Tomography (CT) scans of the thorax are widely applied in diagnose. It is seen that CT scanning gives precise information about the size, shape and location of the tumor and increases the detection rate of pulmonary nodules and is hence considered useful in the detection of pulmonary nodules [10]. These DICOM CT medical images contain the textual information other than the content data. This text information provides the semantic information [3-9]. Low-level features can not entirely describe human recognition to images [3], so satisfying results are not obtained. The role of semantic feature is very important for the prefiltration of the images from the Lung Image Database Consortium (LIDC) [2, 34]. DICOM header [6-9] gives the high level semantic information by using its parameters to perform the preprocessing search, so only relevant images will be searched in the database. The performance of medical image retrieval is increased. The next step of the medical image retrieval system for identifying the lung nodules is lung segmentation [11] [12]. The purpose of the segmentation is to separate human body regions from background and makes an initial classification showing the right and left lung clearly. For the retrieval of lung nodule from the separated lungs area, it is further segmented to extract the exact ROI in the case of cancer detection [14]. Vincent Chu [15] proposed MATLAB based tool called MATITK that uses the watershed algorithm for segmentation but problem was the clear visualization. However, many papers are published on plain rotation invariance analysis [27, 28, 29]. A number of techniques incorporating invariance with respect to both spatial

scale and rotation have been developed [30, 31]. For the segmentation of lung nodules on CT images, Rotation invariant Local Binary Pattern (LBP) [16] has shown very effective results. This helps in clear visualization of nodule boundaries which is important for doctors for analyzing the disease effects. Many LBP and other methods have been stated so far for the segmentation step [16, 17-20] but all of them were used for classification of the lung nodules. The direct implementation of rotation and scale invariance using LBP has not been considered so far. Thus, the technique is used to implement benefits of LBP method into lung cancer imagery with template matching. Different machine learning techniques, including template matching, Support Vector Machines, Linear Discriminant Analysis and linear programming technique are available to match lung nodule characteristics [21] in the retrieval system. For templates without strong features, a template-based approach using Sum of Absolute Differences (SAD) measure is effective [22, 23].

2. HIGH LEVEL FEATURES FROM DICOM CT SCANS

High level semantic features [7] are extracted from the header of DICOM lung CT Scans in the preprocessing step. The information stored in the Digital Imaging and Communications in Medicine (DICOM) images plays important role in the extraction of lung CT images. The semantic meaning is found from the text in the image report of DICOM lung CT images by radiologists [9].

As now DICOM standard format based on National Electrical Manufacturers Association (NEMA) [4, 5] is currently used in medical imaging. DICOM image comprises of many tags. There are around 124 tags in each of DICOM image. Each tag presents the features of the image. Moreover, DICOM contains both a header as well as all of the image data. The DICOM header size varies depending on how much header information is stored. In the header, it stores the textual information of the patient image such as patient name, patient image type, study time, modality, dimensions, slice thickness, slice length etc. Using some features from the header like slice thickness, slice length helps in the extraction of semantic content from an image. The extracted high level semantic information stores in the database which can be used during the retrieval process.

The following portal in figure 1 shows the some parameters of the DICOM header.

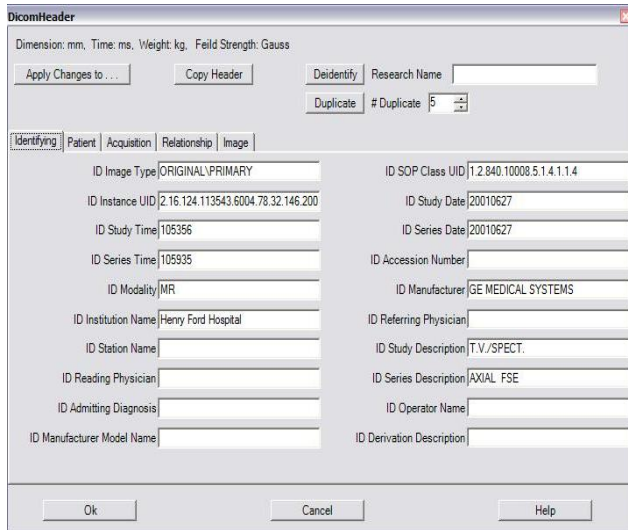


Figure 1. DICOM Header information Portal

3. SEGMENTATION IN MEDICAL IMAGING

Segmentation has an important role in medical imaging as it helps in extracting the organ of interest. For the diagnosis of lungs, it is necessary to segment the chest images and extract the lungs in the preprocessing step and further the nodules are segmented with the different methods. One pulmonary CT image as shown in figure 2 is a precursor to most pulmonary image analysis applications.



Figure 2. The lung Cancer Image in which lung parenchymas seen as the dark region in the body. The surrounding tissue appears with a higher intensity.

By using the following steps, firstly lung fields are separated from background [24] on the filtered lung CT images as shown in figure 3.

1. Optimal Thresholding: The image is thresholded to separate low-density tissue (eg. Lung parenchymas) from fat.
2. Background removal: The surrounding air, identified as low-density tissue, is removed.
3. Cleaning: It is performed to fill the holes in the binary image.
4. Lung mask: To extract lungs from background, lung mask is created.
5. Lung Extraction: Output of step 4 is subtracted from the original image to provide separated lungs for further processing.

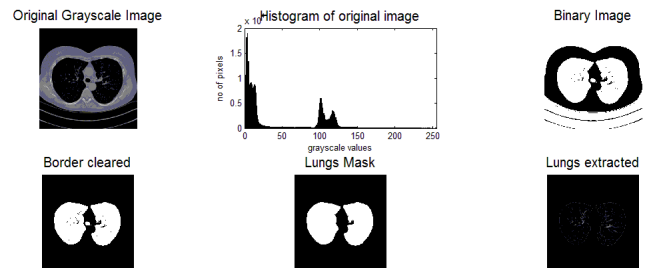


Figure 3. Separation of Lung fields after the removal of mediastinum (a) Original DICOM CT Lung Image from LIDC (b) Thresholding point using histogram (c) Binary Image (d) Cleaning (e) Lung Mask (f) Lungs Extraction

3.1 Rotation Invariant Local Binary Pattern

After getting lung parenchymas from the preprocessing step, rotation invariant and gray scale invariance features using Local Binary Operator is used to get the nodules. This provides efficient segmentation of lung nodules and helps in clear visualization of nodule boundaries which is important for doctors for analyzing the disease effects. The segmented image shows all the nodules clearly but the nodules that benign or malignant cannot be separated or identified by segmentation.

“Local Binary Pattern provides the texture features which can be seen as a unifying approach to the traditionally divergent statistical and structural models of texture analysis [25]. It has become a popular approach in various applications because of its discriminative power and computational simplicity which in turn, makes it possible to analyze images in challenging real-time settings. Moreover, the most important property of the *LBP* operator in real-world applications is its robustness to monotonic gray-scale changes caused, for example, by illumination variations. It labels the pixels of an image by thresholding the neighborhood of each pixel and considers the result as a binary number [26] as shown below in example of 3*3 neighborhoods. Starting from the joint distribution of gray values of a circularly symmetric neighbor set of eight pixels in a 3x3 neighborhood, operator is invariant against any monotonic transformation of the gray scale. The dimensionality of the *LBP* feature distribution is calculated according to the number of neighbors used. The definition of the *LBP* has been extended to arbitrary circular neighborhoods of the pixel to achieve multi-scale analysis and rotation invariance [13, 16, 18]. Rotation invariance is achieved by recognizing the gray scale invariant operator which incorporates a fixed set of rotation invariant patterns” [13, 16].

The value of the *LBP* code of a pixel (x_c, y_c) is given by:

$$LBP_{P,R} = \sum_{p=0}^{P-1} s(g_p - g_c) 2^p, s(x) = \begin{cases} 1, & \text{if } x \geq 0; \\ 0, & \text{otherwise;} \end{cases} \quad (1)$$

Where

g_c : gray value of the center pixel

g_p : gray values of the circularly symmetric neighborhood g_p ($p=0, \dots, P-1$).

P : Image Pixels, circle of radius R ($R > 0$) that form a circularly symmetric neighbor set respectively

2^p : binomial factor for each sign $s(g_p - g_c)$

An example of computing *LBP* and Contrast measure (*C*) in a 3*3 neighborhoods:

example	thresholded	weights																											
<table border="1"> <tr><td>6</td><td>5</td><td>2</td></tr> <tr><td>7</td><td>6</td><td>1</td></tr> <tr><td>9</td><td>8</td><td>7</td></tr> </table>	6	5	2	7	6	1	9	8	7	<table border="1"> <tr><td>1</td><td>0</td><td>0</td></tr> <tr><td>1</td><td>1</td><td>0</td></tr> <tr><td>1</td><td>1</td><td>1</td></tr> </table>	1	0	0	1	1	0	1	1	1	<table border="1"> <tr><td>1</td><td>2</td><td>4</td></tr> <tr><td>128</td><td>32</td><td>8</td></tr> <tr><td>64</td><td>32</td><td>16</td></tr> </table>	1	2	4	128	32	8	64	32	16
6	5	2																											
7	6	1																											
9	8	7																											
1	0	0																											
1	1	0																											
1	1	1																											
1	2	4																											
128	32	8																											
64	32	16																											

Pattern = 11110001

$LBP = 1 + 16 + 32 + 64 + 128 = 241$

$C = (6+7+8+9+7)/5 - (5+2+1)/3 = 4.7$

Important properties are:

- *LBP* is invariant to any monotonic grey level change
- Computational simplicity

To remove the effect of rotation, i.e. to assign a unique identifier to each rotation invariant local binary pattern, rotation invariance is defined, formally:

$$LBP_{p,Rri} = \min \{ROR(LBP_{p,R}, i) | i = 0, \dots, P - 1\} \quad (2)$$

Where $ROR(x, i)$ function performs a circular bit-wise right shift on the P-bit number x , i times.

To quantify the varying performance of individual patterns attributes to the spatial structure of the patterns, a uniformity measure U ('pattern') is defined, which corresponds to the number of spatial transitions (bitwise 0/1 changes) in the 'pattern'. These patterns are called "uniform" because they have one thing in common: at most two one-to-zero or zero-to-one transitions in the circular binary code. However, only limited subsets of 'uniform' patterns are used instead of all rotation invariant patterns, which improve the rotation invariance considerably. So, this operator is called as $LBP_{8,R}^{riu2}$. The use of 'uniform' patterns only is motivated by the reasoning that they tolerate rotation better because they contain fewer spatial transitions exposed to unwanted changes upon rotation.

"The *LBP* operator is an excellent measure of the spatial structure of local image texture, but it discards the other important property of local image texture, contrast, since it depends on the gray scale. If only rotation invariant texture analysis is desired, i.e., gray-scale invariance is not required. The performance of *LBP* is further enhanced by combining it with a rotation invariant variance measure *VAR* that characterizes the contrast of local image texture.

$$VAR_{p,R} = \frac{1}{p} \sum_{p=0}^{p-1} (g_p - \mu)^2, \text{ where } \mu = \frac{1}{p} \sum_{p=0}^{p-1} g_p \quad (3)$$

VAR_8 is invariant against shifts in gray scale. *LBP* and *VAR* are complementary, the joint distributions $LBP_{8,R}^{riu2}/VAR_8$ (aka *LBPV*) is very powerful rotation invariant measure of local image texture" [13, 16]. The rotation invariant *LBP* uniform pattern image $LBP_{1,8}^{riu}$ and correspondingly histogram of the lung segmented nodules showing texture variance features after finding out the uniform pattern in figure 4(a) and 4(b) respectively.

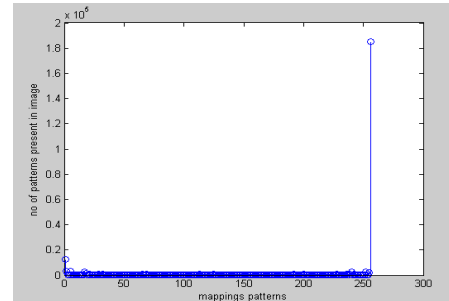
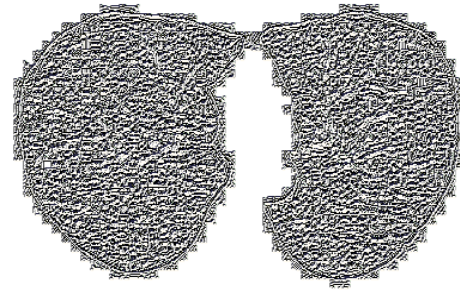


Figure 4. (a) Rotation Invariant LBP Uniform Pattern Image LBP^{riu} (b) Histogram Showing LBP Image using rotation invariant pattern of Image

The final combined operator *LBPV* separates the textures with clear boundaries resulting in very efficient segmentation of image as shown in figure 5.

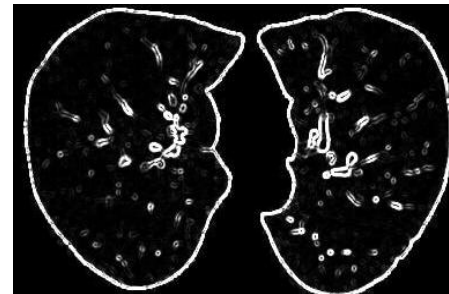


Figure 5. Segmentation of Lung Nodules Using Combined LBPV operator

Using SIENET Sky Dicom viewer tool [32] and RadiAnt DICOM viewer tool [33], segmentation of all the slices of medical images can be viewed efficiently.

4. TEMPLATE MATCHING

To identify the cancer lung nodule from segmented image by *LBP* technique, the different size templates of cancerous nodules are matched by using template matching. "Template matching is a technique in digital image processing for finding small parts of an image which match a template image [22, 35-36]. A basic method of template matching uses a template, tailored to a specific feature of the search image, which is to detect. This technique can be easily performed on grey images or edge images. The output will be highest at places where the image structure matches the mask structure. Template matching uses the intensities of the pixels, using the Sum of Absolute Differences (SAD) measure [23]. A pixel in the search image with coordinates (x_s, y_s) has intensity $I_s(x_s, y_s)$ and a pixel in the template with coordinates (x_t, y_t) has intensity $I_t(x_t, y_t)$. Thus the absolute difference in the pixel intensities is defined as $Diff(x_s, y_s, x_t, y_t) = |I_s(x_s, y_s) - I_t(x_t, y_t)|$.

$$SAD(x, y) = \sum_{i=0}^{T_{rows}} \sum_{j=0}^{T_{cols}} Diff(x + i, y + j, i, j) \quad (4)$$

In this method, the lowest SAD score gives the estimate for the best position of template within the search image [22]. The technique is simple to implement and understand in particular lung medical imaging.

5. CONCLUSIONS

Different methods used in Content based medical lung image retrieval are defined in this paper that can be used for efficient visualization as well as automatically extracting the lung nodules from lung CT data. The combination of high level features from DICOM CT with low level features by LBP is used. Retrieval is performed first by extracting semantic information from the dataset values of the DICOM header which produces a set of filtered images. The set of images obtained after searching through the dataset values, rotational invariant linear binary pattern is applied to perform the segmentation of the lung nodules. Template matching using the Sum of Absolute Differences (SAD) measure is discussed to extract abnormal nodules from segmented images with standard template nodules.

REFERENCES

- [1] American Cancer Society. Factbox: Latest U.S. cancer statistics (2011). American Cancer Society, Atlanta, GA. <http://www.reuters.com/article/2011/06/17/us-factbox-cancer-idUSTRE75G0PL20110617>
- [2] United States National Institute of Health www.nih.gov
- [3] Muller H, Michoux N, Bandon D, Geissbuhler A, (2004) "A review of content-based image retrieval systems in medical applications-clinical benefits and future directions", *Int J Med Inform*, Vol.73(1), pp.1-23.
- [4] Digital Imaging and Communications in Medicine (DICOM) - Part 1: Introduction and Overview, DICOM PS 3.1, *National Electrical Manufacturers Association - NEMA*. Rosslyn, Virginia, USA. 2004.
- [5] Bas Revet, (1997) *DICOM Cook Book for Implementations in Modalities*, Nederland: Philips Medical Systems.
- [6] Antonio da Luz Jr., Daniel D. Abdala, Aldo v. Wangenheim, Eros Comunello, (2006) "Analyzing DICOM and non-DICOM Features in Content-Based Medical Image Retrieval: A Multi-Layer Approach", *Proceedings of the 19th IEEE Symposium on Computer-Based Medical Systems (CBMS'06)*, pp. 93-98.
- [7] A. Grace Selvarani, S. Annadurai, (2007) "Medical image retrieval by combining low level features and DICOM features", *IEEE International Conference on Computational Intelligent and Multimedia Applications*, Vol. 1, pp. 587 – 589.
- [8] Sheng Wu, Yi Xue, Gong Cheng, Xue Za Zhi, (2009) "Medical image retrieval by high level semantic features and low level content features of image", *PubMed - indexed for MEDLINE*, Vol.26(6), pp.1237-40.
- [9] Hong Shao, Wen-cheng Cui, Hong Zhao, (2004) "Medical image retrieval based on visual contents and text information", *IEEE International Conference on Systems, Man and Cybernetics*, Vol.1, pp.1098-1103.
- [10] M. Prokop I. Sluimer, A. Schilham, B. van Ginneken, (2006) "Computer analysis of computed tomography scans of the lung: A survey", *IEEE Transactions on Medical Imaging*, Vol.25(4), pp.385-405.
- [11] Pradeep Singh, Sukhwinder Singh, Gurjinder Kaur, (2008) "A Study of Gaps in CBMIR using Different Methods and Prospective", *Proceedings of world academy of science, engineering and technology*, Vol. 36, ISSN 2070-3740, pp. 492-496.
- [12] Zhen Ma, João Manuel R. S. Tavares, R. M. Natal Jorge, (2009) "A review on the current segmentation algorithms for medical images", 1st International Conference on Imaging Theory and Applications (IMAGAPP), Lisboa, Portugal, *INSTICC Press*, pp. 135-140.
- [13] Ojala, T., Pietikäinen, M., Mäenpää, T., (2000) "Gray Scale and Rotation Invariant Texture Classification with Local Binary Patterns", *Lecture Notes in Computer Science*, Vol. 1842, pp. 404-420.
- [14] Alexander S. Behnaz, James Snider, Chibuzor Eneh et.al, (2010) "Quantitative CT for Volumetric Analysis of Medical Images: Initial Results for Liver Tumors", *Medical Imaging 2010, Proc. of SPIE*, Vol 7623-76233U.
- [15] Vincent Chu and Ghassan Hamarneh, (2006) "MATLAB-ITK Interface for Medical Image Filtering, Segmentation and Registration", *Medical Imaging 2006: Image Processing, Proc. of SPIE*, Vol. 6144, 61443T1-8.
- [16] Ojala, T., Pietikäinen, M., Mäenpää, T., (2002) "Multiresolution gray-scale and rotation invariant texture classification with Local Binary Patterns", *IEEE Transaction*, Vol. 24, pp.971–987.
- [17] Edward H.S. Lo, Mark R. Pickering, Michael R. Frater, John F. Arnold, (2011) "Image segmentation from scale and rotation invariant texture features from the double dyadic dual-tree complex wavelet transform", *Image and Vision Computing (ELSEVIER)*, Vol. 29 (1), pp. 15-28.
- [18] Pietikäinen, M., Ojala, T., Xu, Z., (2000) "Rotation-Invariant texture classification using feature distributions", *Pattern Recognition*, Vol. 33, pp. 975-985.
- [19] Zhenhua Guo, Lei Zhang, David Zhang, (2010) "Rotation invariant texture classification using LBP variance (LBPV) with global matching", *Biometrics Research Centre, Department of Computing, The Hong Kong Polytechnic University, Hung Hom, Kowloon, Hong Kong, China, Pattern Recognition*, Vol. 43, pp.706–719.
- [20] Timo Ojala, Matti Pietikanen, (1999) "Unsupervised texture segmentation using feature distributions", *Machine Vision and Media Processing Group, Pattern Recognition*, Vol. 32, pp.477-486.
- [21] Caifeng Shan, Shaogang Gong, Peter W. McOwan, (2009) "Facial expression recognition based on Local Binary Patterns: A comprehensive study", *Image and Vision Computing*, Vol. 27, pp. 803–816.
- [22] Fredriksson, K., (2001) "Rotation Invariant Template Matching", *TECHREPORT, PhD Thesis, A-2001-3*, pp.139.
- [23] Alsaade, F., (2012) "Fast and Accurate Template Matching Algorithm Based on Image Pyramid and Sum of Absolute Difference Similarity Measure", *Research Journal of Information Technology*, Vol. 4, pp. 204-211.
- [24] Heuberger, J., Geissbuhler, A., Muller, H., (2005) "Lung CT segmentation for image retrieval using the

- Insight Toolkit (ITK)", *Medical Imaging and Telemedicine, (MIT2005)*. Hopitaux University of Geneva, China.
- [25] Ojala, T., Pietikäinen, M., Harwood, D., (1996) "A Comparative Study of Texture Measures with Classification Based on Feature Distributions", *Pattern Recognition*. Vol. 29, pp. 51-59.
- [26] Haralick, R.M., (1979) "Statistical and structural approaches to Texture", *Proc IEEE 67*. Vol.5, pp.786-804.
- [27] Lam, W.-K., Li, C.-K., (1997) "Rotated Texture Classification by Improved Iterative Morphological Decomposition", *IEE Proc. - Vision, Image and Signal Processing*. Vol.144, pp.171-179.
- [28] Madiraju, S.V.R., Liu, C.C., (1995) "Rotation Invariant Texture Classification Using Covariance", *Proc. Int. Conf. Image Processing*. pp. 262-265.
- [29] Mao, J., Jain, A.K., (1992) "Texture Classification and Segmentation Using Multiresolution Simultaneous Autoregressive Models", Vol. 25, pp.173-188.
- [30] Wu, Y., and Yoshida, Y., (1995) "An Efficient Method for Rotation and Scaling Invariant Texture Classification", *Proc. IEEE Int'l Conf Acoustics, Speech, and Signal Processing*, Vol.4, pp. 2519-2522.
- [31] Wu, Y., and Yoshida, Y., (1995) "An Efficient Method for Rotation and Scaling Invariant Texture Classification", *Proc. IEEE Int'l Conf Acoustics, Speech, and Signal Processing*, Vol.4, pp. 2519-2522.
- [32] Siemens Corporation, "SIENET Sky – DICOM CD Viewer"
<http://www.webbuyersguide.com/Product/viewproduct.aspx?id=42372>
- [33] Maciej Frankiewicz, "http://www.radiantviewer.com/", Poland.
- [34] Kascic, E., NBIA - National Cancer Imaging Archive NCIA (version 4.0): The NCI's repository for DICOM-based images (<https://cabig.nci.nih.gov/tools/NCIA>)
- [35] H. Y. Kim and S. A. Araújo, (2007) "Grayscale Template-Matching Invariant to Rotation, Scale, Translation, Brightness and Contrast", *IEEE Pacific-Rim Symposium on Image and Video Technology, Lecture Notes in Computer Science*, Vol.4872, pp.100-113.
- [36] Ashley Aberneithy, (2007) "Automatic Detection of Calcified Nodules of Patients with Tuberculous", University College, London.